Optics and Spectroscopy, 2023, Vol. 131, No. 2

02

Kinetics of reversible phase transitions in $Ge_2Sb_2Te_5$ thin films at femtosecond laser irradiation

© *A.V. Kolchin*[1], *S.V. Zabotnov*[2], *D.V. Shuleiko*[2,3], *P.I. Lazarenko*[4], *V.B. Glukhenkaya*[4],
S.A. Kozyukhin[1], *P.K. Kashkarov*[2,5]

[1] Kurnakov Institute of General and Inorganic Chemistry, Russian Academy of Sciences,
119991 Moscow, Russia
[2] Department of Physics, Moscow State University,
119991 Moscow, Russia
[3] NTI Competence Center for Big Data Storage and Analysis, Lomonosov Moscow State University,
11999 Moscow, Russia
[4] National Research University „Moscow Research Institute of Electronic Technology “,
Institute of Advanced Materials and Technologies,
124498 Zelenograd, Moscow, Russia
[5] National Research Center „Kurchatov Institute“,
123182 Moscow, Russia
e-mail: avkolchin@physics.msu.ru

Received December 01, 2022
Revised December 23, 2022
Accepted January 28, 2023

Femtosecond laser irradiation of amorphous $Ge_2Sb_2Te_5$ thin films initiates reversible phase transitions. The amorphization and crystallization of $Ge_2Sb_2Te_5$ thin films were experimentally and theoretically confirmed. Electron and lattice temperatures kinetics during laser pulse duration were evaluated by two-temperature models calculations and experimental data. The dynamical changing of optical properties have been taking into account. Temperatures and cooling rates, which are necessary to initiate phase transitions by IR laser pulses with subpicosecond duration. The observed results open perspectives for improvement of $Ge_2Sb_2Te_5$ nanophotonical devices.

Keywords: $Ge_2Sb_2Te_5$ femtosecond laser technologies, Raman spectroscopy, phase transitions.

DOI: 10.21883/0000000000

Introduction

Chalcogenide semiconductor $Ge_2Sb_2Te_5$ (GST225) is widely used as a basic material for the development of nonvolatile read-write memory devices [1]. In-particular, GST225 is used in DVD−RW and PC−RAM due to the reversible phase transitions. The amorphous and crystalline phases demonstrate significant contrast between optical and electrophysical properties which allows to write, store and read data. Laser pumping is one of the methods of data writing and rewriting operations.

In case of continuous laser irradiation, crystallization of initial amorphous GST225 films flows within at least 100 ns [2]. This time is necessary for nucleation in the amorphous matrix [3]. At the same time crystallization of amorphous GST225 is accompanied by reconfiguring of germanium atoms in the lattice [4]. Thus, it is possible at relatively low temperatures from 400 K to 500 K [5].

Currently, research community is focused on crystallization of amorphous GST225 during minimum possible times in order to improve the response of data media based on this material. This is required for successful competition with existing DRAM and flash memory formats [6]. The transition from nanosecond laser pulses to femtosecond pulses for GST225 phase switching is a promising approach to achieve a qualitative leap in further development of devices based on phase-changing materials [7]. Thus in the article [8] have been shown that the minimum time for electron and lattice temperature equalizing in GST225 when heated with ultrafast laser pulses sufficient for transition from amorphous state to crystalline state is 80 ps, which constitutes a high utilization potential of this material for fast data writing in this way. It should be noted that the cooling rate of GST225 shall not exceed 300 K/ns in order to form a crystalline phase [9].

On the other hand, memory erasing in GST225-based devices implemented by means of reverse phase transition — amorphization [1] — is performed by means of heating crystallized areas up to a melting temperature of 880 K followed by cooling at a rate of 10 K/ns and higher [10]. Such conditions may be achieved by fitting femtosecond laser pulse widths and energy provided that suitable GST225 film thicknesses and types of substrates are selected which also influence the phase transition kinetics [11].

Despite the large amount of experimental and theoretical findings, reversible phase transitions in thin GST225 films are studied and calculations are compared with observations primarily without accurate matching of numerical and experimental parameters to each other. The purpose of this study is to experimentally identify the potential for phase transition initiation from amorphous to crystalline state and back in thin GST225 films when exposed to femtosecond laser pulses and analyze the dynamics of such processes using a two-temperature simulation with calculation of experimental parameters of samples and different laser emission modes.

Experimental methods

Thin amorphous GST225 films on preliminary thermally oxidized crystalline silicon substrates were made by magnetron sputtering (MVU TM Magna 10) of a polycrystalline target (ACI Alloys). Silicon oxide layer thickness (SiO_2) was 1000 ± 40 nm, and GST225 thickness was 200 ± 20 nm. Argon pressure in the chamber before and during sputtering was $3 \cdot 10^{-3}$ and $5.7 \cdot 10^{-1}$ Pa, respectively.

Phase transitions in deposited films were induced by emission generated by Avesta femtosecond laser system (wave length $\lambda = 1250$ nm, pulse width $\tau = 135$ fs, repetition rate $\nu = 10$ Hz, pulse energy $E = 10\,\mu$J). The samples were irradiated in air with laser beam scanning of GST225 film surface at normal incidence and focusing with 8 cm lens. Laser energy fluence in these conditions was $F \approx 0.1$ J/cm^2.

The scanning mode was implemented using Standa automated mechanical translators. The samples were moved in one direction along the laser emission polarization vector orientation at rate $V = 5$ or $20\,\mu$m/s. As a result,single scan lines with a width equal to laser spot diameter $d = 100\,\mu$m. For this, the number of laser pulses N_s acting on the unit area of the sample during exposure in each case calculated using the following equation

$$N_s = \frac{\nu d}{V}. \tag{1}$$

Exposures calculated using expression (1) are $N_s = 200$ and $N_s = 50$, respectively. Variation of N_s allowed to implement both initial amorphous GST225 film crystallization mode and reamorphization mode by means of longer irradiation.

The images of irradiated surfaces were obtained by means of optical microscopy (OM, Olympus BX41). Phase composition of initial and irradiated films was determined using the Raman spectra analysis findings measured using Horiba Jobin Yvon HR800 spectrometer. The excitation wavelength was 488 nm, integration time was 40 s and the number of measurements was 16.

Theoretical modeling

Irradiation of semiconductors by femtosecond laser pulses is known to facilitate photoinduced generation of free charge carriers [12]. Concentration of charge carriers $n_e(x,t)$ generated in the irradiated GST225 film may be calculated by solution of the following differential equation:

$$\frac{\partial n_e}{\partial t} - D\frac{\partial^2 n_e}{\partial x^2} = \frac{\alpha(1-R)I(x,t)}{\hbar\omega} + \frac{\beta(1-R)^2 I^2(x,t)}{2\hbar\omega} - \frac{n_e}{\tau_{ee}}, \tag{2}$$

where D is the ambipolar diffusion coefficient, ω is the laser frequency, R is the optical reflectance, $I(x,t)$ is the dependence of incident laser emission intensity on time t and film depth x, α and β are the one- and two-photon absorption coefficients of GST225, respectively. Axis OX is directed from the film surface to its interface with the substrate. Electron-electron collision time τ_{ee} is calculated [13] using the following equation

$$\tau_{ee} = \frac{\mu m^*}{e}, \tag{3}$$

where μ is the charge carrier mobility, m^* and e is the effective electron mass and charge, respectively. $I(x,t)$ used in (2) is calculated using the following equation:

$$I(x,t) = I(t)\exp(-\alpha x) + \frac{I(t)}{1+\beta x I(t)}, \tag{4}$$

taking into account one- and two-photon absorption of GST225 and laser pulse shape $I(t)$ described as

$$I(t) = I_0 \exp\bigl(-(t-\tau/2)^2/\tau^2\bigr), \tag{5}$$

where τ is the laser pulse width. As shown, free electron concentration n_e changes in a dynamic manner depending on the time and position in the environment/thin film/substrate system. As a consequence, according to Drude theory, permittivity of the film material ε^*, linear optical absorption α^* and reflectance R^* included in equation (2) vary:

$$\varepsilon^*(x,t) = \varepsilon - \frac{4\pi e_0^2 n_e(x,t)}{m^*\varepsilon_0(\omega^2 + \tau_{ee}^{-2})}, \tag{6}$$

$$\alpha^*(x,t) = \frac{2\omega}{c}\,\mathrm{Im}\,\varepsilon^*(x,t), \tag{7}$$

$$R^*(x,t) = \left|\frac{\sqrt{\varepsilon^*(x,t)}-1}{\sqrt{\varepsilon^*(x,t)}+1}\right|^2. \tag{8}$$

Dynamic variation of optical properties of amorphous and crystalline GST225 such as reflectance and linear absorption considerably influences the ultrashort laser pulse impact within the pulse width. In this case, the specific absorption rate from an external heat source is recorded as follows [14]:

$$S(x,t) = \alpha^*(x,t)\bigl(1-R^*(x,t)\bigr)I(x,t) + \beta\bigl(1-R^*(x,t)\bigr)^2 I^2(x,t). \tag{9}$$

In addition, excitation of free charge carriers as a result femtosecond laser irradiation dramatically impacts the mechanism of GST225 heating. This is associated with plasma thermalization and following relaxation of the energy absorbed by free electrons into a crystalline lattice [14]. The system of interconnected heat transfer equations for free electrons and lattice is written as follows:

$$\rho c_e \frac{\partial T_e}{\partial t} = k_e \frac{\partial^2 T_e}{\partial x^2} - g(T_e - T_l) + S(x,t), \tag{10}$$

$$\rho c_l \frac{\partial T_l}{\partial t} = k_l \frac{\partial^2 T_l}{\partial x^2} + g(T_e - T_l), \tag{11}$$

where ρ is the substance density, c_e and k_e are the electronic heat capacity and electron heat conductivity coefficient, g is the electron-lattice relaxation constant, c_l and k_l are the lattice heat capacity and heat conductivity coefficient, T_e and T_l are the electron and lattice temperatures, respectively. c_e and k_e depend on free charge carrier concentration $n_e(x,t)$ calculated using equation (2) and are calculated as follows:

$$c_e = \frac{3}{2} k_b n_e, \tag{12}$$

$$k_e = \frac{8k_b^2}{3\pi m^*} n_e T_e, \tag{13}$$

where $k_b = 1.38 \cdot 10^{-23}$ J/K is Boltzmann constant. Electron lattice relaxation constant is calculated as

$$g = \frac{c_e}{\tau_{e-h}}, \tag{14}$$

where τ_{e-h} is the electron lattice relaxation time. system of equations (2)−(14) was numerically solved by the method of finite differences in MatLab software using a rectangular grid. The initial conditions used in the calculations are $n_e = 0\,\text{cm}^{-3}$ and $T_e = T_l = 293\,\text{K}$ at $t = 0$. Time t is counted from the start of film irradiation to the laser pulse. Calculations by a coordinate and time used increments $\Delta x = 1$ nm and $\Delta t = 1$ fs,respectively. Physical quantities used in the numerical simulation are listed in the table.

Values used in the calculations within the thermal process behavior simulation when amorphous thin GST225 films are exposed to femtosecond laser pulses

Permittivity of nonirradiated amorphous GST225 (ε)	$18.2 + 2.06$i [15]
Permittivity of nonirradiated crystalline GST225 (ε)	$45.3 + 28.3$i [15]
Optical reflectance of amorphous GST225 (R)	0.36 [15]
Optical reflectance of FCC crystalline GST225 (R)	0.58 [15]
Linear optical absorption of amorphous GST225 (α)	$24\,500\,\text{cm}^{-1}$ [15]
Linear optical absorption of crystalline GST225 (α)	$185\,000\,\text{cm}^{-1}$ [15]
Nonlinear optical absorption GST225 (β)	0.5 cm/GW [16]
Effective mass (m^*)	$0.68m_0$ [17]
Charge mobility (μ)	$52\,\text{cm}/(\text{V}\cdot\text{s})$ [17]
Ambipolar diffusion coefficient (D)	$2\,\text{cm}^2/\text{s}$ [7]
Electron-phonon relaxation time (τ_{e-h})	2 ps [18]
DensityGST225 (ρ)	$6 \cdot 10^3\,\text{kg/m}^3$ [18]
GST225 lattice heat capacity (c_l)	$220\,\text{J}/(\text{kg}\cdot\text{K})$ [18]

Results and discussion

OM images (Figure 1) obtained in reflected light show that nonirradiated areas on thin GST225 films are dark [11].

While the area exposed to femtosecond laser pulse sequence with $N_s = 50$ (Figure 1, a) becomes lighter that may be indicative of its crystallization [11], because the reflectance of crystalline GST225 in visible range 400−800 nm is higher by $\Delta R = 0.3$ than that of amorphous GST225 [15].

Analysis of irradiated and nonirradiated areas by Raman spectroscopy method has shown the following differences. Raman spectrum of initial GST225 film constitutes an asymmetric wide band in the wave number range $100-250\,\text{cm}^{-1}$ (Figure 2, a). This wide band in the spectrum is caused by the short-range order of amorphous GST225 phase and is a sequence of signal overlapping from five lines [19] with peaks near 126, 141, 158, 190 and $215\,\text{cm}^{-1}$. Lines near 126, 190 and $215\,\text{cm}^{-1}$ are associated with oscillation mode A_1 of $GeTe_{4-n}Ge_n$ tetrahedra ($n = 1, 2$) [20]. In this case, the line near $215\,\text{cm}^{-1}$ can also correspond to mode F_2 of $GeTe_4$ tetrahedra [20]. Other lines are caused by the contribution of Sb_2Te_3: peak near $141\,\text{cm}^{-1}$ pertains to pyramidal structural units Sb_2Te_3 [21] and the line near $158\,\text{cm}^{-1}$ corresponds to mode A_{1g}^2 of Sb_2Te_3 structure. Raman spectra of samples irradiated at $N_s = 50$ are also an asymmetric wide band in the range of $100-250\,\text{cm}^{-1}$ (Figure 2, b), which is decomposed into 5 lines in a similar way. However, as shown in Figure 2, intensity ratio between these lines differs. In particular signal drop from the line near $158\,\text{cm}^{-1}$ and integral intensity growth of line decreases near $126\,\text{cm}^{-1}$ and $141\,\text{cm}^{-1}$ are observed. These changes may indicate crystallization of amorphous GST225 film into a face-centered cubic (FCC) crystalline phase due to reconfiguration of $GeTe_4$ structural units. Such phase transitions of GST225 from the amorphous state to the crystalline phase [21] may be achievable at temperatures above 410 K [5].

During longer irradiation in a mode with $N_s = 200$ (Figure 1, b), the same dark area appears in the center of the scan line as in nonirradiated film areas. This effect can be caused by reamorphization [11]. Additionally, surface lattices with a constant approximately equal to a structuring emission wavelength and with orientation perpendicular to

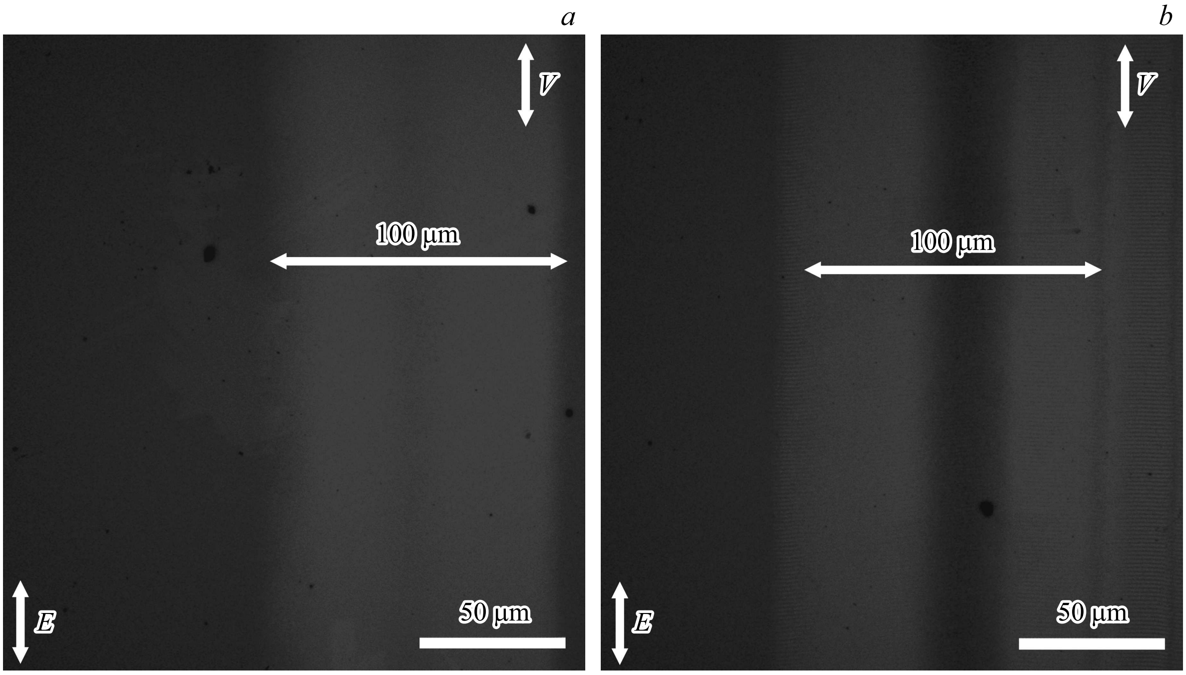

Figure 1. Optical images of thin GST225 films irradiated by $N_s = 50$ (a) and $N_s = 200$ (b) femtosecond laser pulses with energy density 0.1 J/cm^2.

the structuring emission polarization are observed. They are the result of interference of surface plasmon-polaritons with incident emission generated at intensive photoexcitation [22]. The following changes are observed in Raman spectrum in the laser scan line center. Integral intensity of line decreases near $126\,\mathrm{cm}^{-1}$, while integral intensity of lines near $141\,\mathrm{cm}^{-1}$ and $158\,\mathrm{cm}^{-1}$ grows, on the contrary (Figure $2, c$). Thus, Raman spectrum becomes similar to the initial nonirradiated GST225 (Figure $2, a$), which together with the optical reflectance variation shown using OM may say for reamorphization when the number of exposing laser pulses is increased [22]. Thus, as a result of femtosecond laser pulse exposure, a reversible phase transition is probably observed, which is implemented by means of heating above a GST225 melting temperature of 880 K in accordance with [10] followed by cooling with a rate higher than 10 K/ns.

The assumptions on crystallization and reamorphization of thin GST225 film in various femtosecond laser pulse exposure modes may be theoretically supported by means of electron and lattice temperature profile analysis within a two-temperature model [14,23] using the calculation method described in „Theoretical Simulation“ section.

The numeric simulation (Figure $3, a$) has shown that simultaneous electron and lattice temperature increase is observed on the surface of amorphous thin GST225 film ($x = 0\,\mathrm{nm}$) at $N_s = 50$ during 300 fs after the beginning of laser pulse exposure. At this time, the lattice temperature achieves its peak of 510 K. According to [5,24], the measured value is higher than the temperature of amorphous GST225 transition into FCC crystalline phase (410 K). Then the lattice temperature starts decreasing at a rate of 80 K/ns (Figure $3, c$). At the same time, the electron temperature, on the contrary, continues to show growth up to 550 K that is achieved at 800 fs. At this time, solution of equation (2) shows that at this time $n_e(0\,\mathrm{mm},\ 800\,\mathrm{fs}) \approx 0$. This may be explained by thermalization of phoexcited charge carries, including by means of collision between free electrons [25] with typical time in GST225 of about 200 fs [13]. A similar trend, but with lower temperatures, is also observed at the thin film and substrate interface at $x = 200\,\mathrm{nm}$ (Figure $3, b$). The lattice temperature increases up to about 440 K during 300 fs after the start of laser pulse exposure. The achieved temperature as at $x = 0\,\mathrm{nm}$ exceeds the temperature of amorphous GST225 transition into FCC crystalline phase 410 K, which demonstrates that crystallization throughout the film thickness is possible at the specified laser emission parameters. This takes place because the penetration depth of the optical emission with a wavelength of 1250 nm $1/\alpha \approx 400\,\mathrm{nm}$ [15] in amorphous GST225 is more than the film thickness. Further lattice cooling takes place with the rate of about 60 K/ns (Figure $3, c$). At the same time, electron temperature at $x = 200\,\mathrm{nm}$ $t = 800\,\mathrm{fs}$ after the start of laser pulse exposure achieves 505 K and then starts decreasing like in case when the surface temperature varies at $x = 0\,\mathrm{nm}$ (Figure $2, b$).

The obtained findings show slow cooling of the irradiated system, which additionally contributes to crystallization of a chalcogenide compound [6]. Cooling down to the threshold crystallization temperature (410 K) takes place during about 1 ns throughout the film thickness (Figure $3, a, b$). Nevetherless, the crystallization process itself may flow faster:

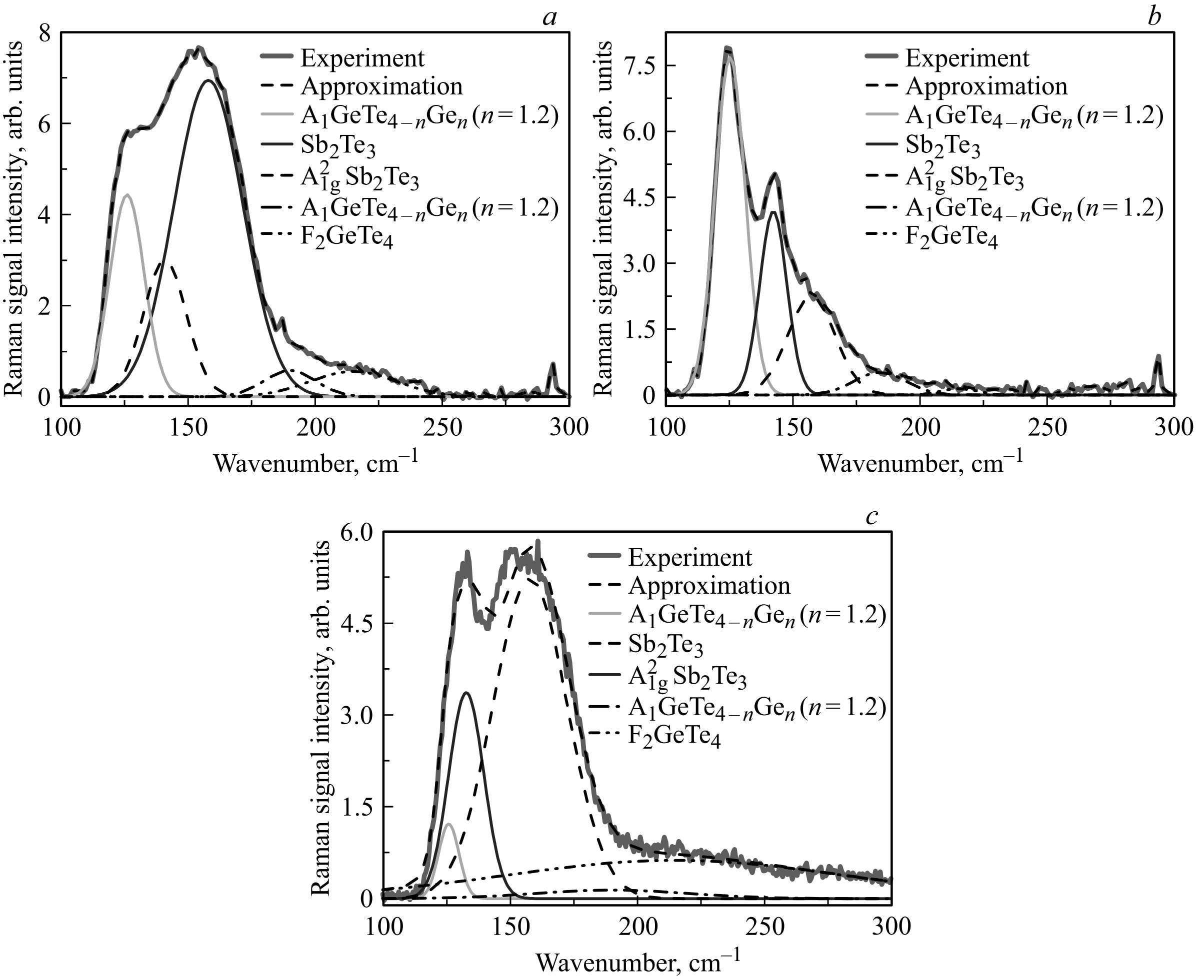

Figure 2. Raman spectra of thin GST225 films before (*a*) and after irradiation with $N_s = 50$ (*b*) and $N_s = 200$ (*c*) femtosecond laser pulses with energy density 0.1 J/cm^2.

according to the recent optical reflectance measurements using the „pump–probe" method [7], crystallization in thin GST225 films as a result of femtosecond laser irradiation may be observed in times of about 100 ps, which is by three orders of magnitude lower than for crystallization with continuous laser exposure [2].

The calculations within the two-temperature model also made it possible to describe the potential reamorphization kinetics of previously crystallized areas on thin GST225 films during exposure to a greater amount of laser pulses $N_s = 200$, when heating is simulated for already crystallized area whose absorption is significantly higher than for amorphous phase (table) resulting in higher heating. In particular, on the thin film surface ($x = 0$ nm), crystalline GST225 lattice is heated up to ≈ 915 K during $t = 600$ fs after the start of laser pulse exposure (Figure 4, *a*). This value exceeds the melting temperature of GST225 (880 K) [23] whose achievement is one of the amorphization process conditions [2]. Then the melt is cooled at a rather high rate of 250 K/ns, which by an order of magnitude higher than the required amorphization value 10 K/ns (Figure 4, *c*) [10]. Due to the high cooling rate and difference in 35 K between the maximum lattice temperature and melting temperature, amorphous layer is hardened during ~ 100 ps, which corresponds to time limits of optical characteristic switching as a result of phase transitions in GST225 [7]. At the same time, at the film and substrate interface ($x = 200$ nm), crystalline GST225 lattice is heated only to about 770 K (Figure 4, *b*), which is lower than the melting temperature of GST225, and this means that reamorphization of crystalline GST225 throughout the film depth is impossible, though the cooling rate remains rather high and exceeds 170 K/ns within the interval of some picoseconds (Figure 4, *c*). This is due to the fact that the penetration depth of 1250 nm optical emission in FCC crystalline phase of GST225 is $1/\alpha \approx 20$ nm [15], which is considerably lower than for amorphous GST225. Thus, the incident laserirradiation is intensively absorbed in the surface region and transition of FCC crystalline phase of GST225 into amorphous state is only possible at a shallow depth of the thin film.

The problem of partial crystallization throughout the depth could be solved by means of increase in the

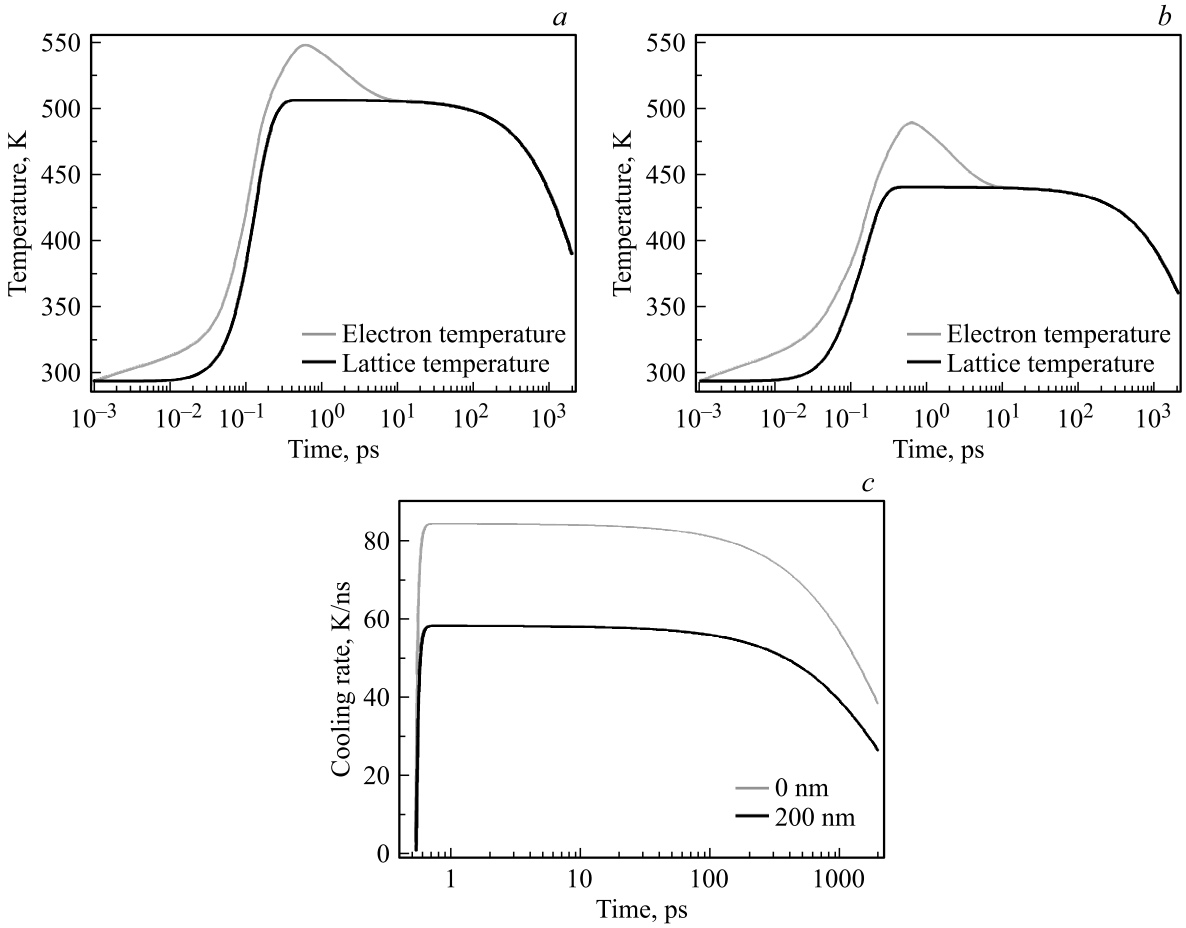

Figure 3. Time dependences of electron and lattice temperatures on the thin film surface at $x = 0$ nm (a) and at the substrate interface at $x = 200$ nm (b) when amorphous thin GST225 films are exposed to $N_s = 50$ laser pulses with energy density $F = 0.1$ J/cm^2; lattice temperature decrease rate on the film surface and substrate interface (c).

structuring emission energy flux density and corresponding increase in the maximum lattice heating temperature. However, in this case the melt cooling down time lower than the amorphous phase transition temperature would also increase. Nevertheless, it should be noted that the performed cooling down time calculations for crystallization and amorphization processes are upper estimates for phase transition time and optical properties change time of thin GST225 films as a result of femtosecond laser irradiation.

Conclusions

The investigation has shown that phase transitions into crystalline state and reversible transition into amorphous phase are possible in initially amorphous thin GST225 films exposed to various number of femtosecond laser pulses. The obtained result is experimentally supported by the Raman spectra analysis and OM images and is theoretically supported by the two-temperature simulation using the laser pulse characteristics and GST225 parameters in amorphous and crystalline phases for calculations. Electron and lattice temperature kinetics analysis shows that, depending on the irradiation mode at subpicosecond times, thin GST225 film can be heated to the temperatures above the threshold of 410 K for transition into FCC crystalline phase or above 880 K for melting followed by fast hardening into amorphous state. The typical thin film cooling down times below these thresholds are within 100 ps–1 ns depending on the irradiation mode, which is indicative of possible decrease in times of the described phase transitions by 2–3 orders compared with the well-studied continuous laser emission application.

The findings are of interest for the development of new techniques of data writing and rewriting in thin GST225 films when exposed to femtosecond laser pulses.

Funding

The investigations of the structural properties of irradiated specimens and simulation of phase transition kinetics were supported by RFBR Grant № 20-32-90111. The specimens of amorphous thin GST225 films were formed in the research laboratory „Active Photonics Materials and Devices“ with the support of the Ministry of Science and

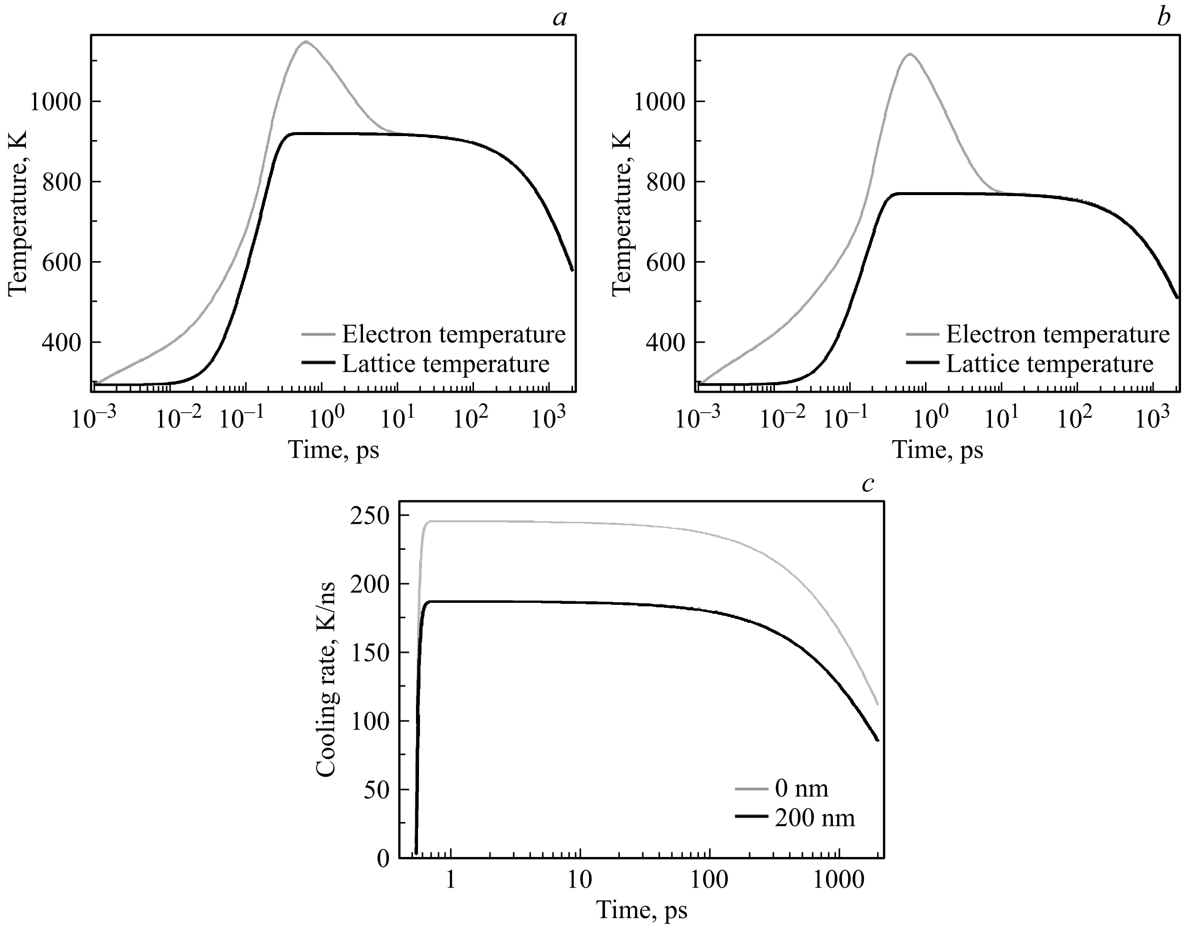

Figure 4. Time dependences of electron and lattice temperatures on the thin film surface at $x = 0$ nm (a) and at the substrate interface at $x = 200$ nm (b) when laser-crystallized thin GST225 films are exposed to $N_s = 200$ laser pulses with energy density $F = 0.1$ J/cm^2; lattice temperature decrease rate on the film surface and substrate interface (c).

Higher Education of the Russian Federation (Agreement № 075-03-2022-212/4 as of 08.11.2022, FSMR-2022-0001). Selection of the optimum specimen irradiation strategies and corresponding modernization of a femtosecond laser system for initiation of phase transitions were performed within the project „New Approaches to Readout System Design for Three-Dimensional Optical Memory Technology with Multilevel Coding“ supported by the Ministry of Science and Higher Education of the Russian Federation under the Agreement between Lomonosov Moscow State University and National Technology Initiative Project Support Foundation as of 15.12.2021. № 70-2021-00252.

Conflict of interest

The authors declare that they have no conflict of interest.

References

[1] S.A. Kozyukhin, P.I. Lazarenko, A.I. Popov, I.L. Eremenko. Russ. Chem. Rev., **91** (9), RCR5033 (2022). DOI: 10.1070/RCR5033.

[2] V. Weidenhof, I. Friedrich, S. Ziegler, M. Wuttig. J. Appl. Phys., **89**, 3168 (2001). DOI: 10.1063/1.1351868

[3] Y. Vorobyov, P. Lazarenko, A. Sherchenkov, N. Vishnyakov, A. Ermachikhin, S. Kozyukhin. J. Phys.: Condens. Matter., **32**, 355401 (2020). DOI: 10.1088/1361-648X/ab8c8a

[4] J. Tominaga, T. Shima, P. Fons, R. Simpson, M. Kuwahara, A. Kolobov. Jpn. J. Appl. Phys., **48**, 03A053 (2009). DOI: 10.1143/JJAP.48.03A053

[5] A.A. Sherchenkov, S.A. Kozyukhin, P.I. Lazarenko, A.V. Babich, N.A. Bogoslovskiy, I.V. Sagunova, E.N. Redichev. Semiconductors, **51**, 146–152 (2017). DOI: 10.1134/S1063782617020191.

[6] N.A. Bogoslovskiy, K.D. Tsendin. Semiconductors, **46**, 559 (2012). DOI: 10.1134/S1063782612050065.

[7] H. Wu, W. Han, X. Zhang. Materials, **15**, 6760 (2022). DOI: 10.3390/ma15196760

[8] Y.H. Wang, F.R. Liu, W.Q. Li, T. Fan, J.F. Yang, Z.M. Wang, F. Liu, N.X. Sun. J. App. Phys., **122**, 043104 (2017). DOI: 10.1063/1.4993451

[9] T. Kunkel, Y. Vorobyov, M. Smayev, P. Lazarenko, A. Romashkin, S. Kozyukhin. Materials Science in Semiconductor Processing, **139**, 10350 (2022). DOI: 10.1016/j.mssp.2021.106350

[10] N. Yamada, E. Ohno, K. Nishiuchi, N. Akahira, M. Takao. J. Appl. Phys., **69**, 2849 (1991). DOI: 10.1063/1.348620

[11] T. Kunkel, Y. Vorobyov, M. Smayev, P. Lazarenko, V. Veretennikov, V. Sigaev, S. Kozyukhin. J. Alloys and Compounds, **851**, 156924 (2021). DOI: 10.1016/j.jallcom.2020.156924

[12] G.A. Martsinovsky, G.D. Shandybina, Yu.S. Dement'eva, R.V. Dyukin, S.V. Zabotnov, L.A. Golovan', P.K. Kashkarov. Semiconductors, **43**, 1298 (2009). DOI: 10.1134/S106378260910008X.

[13] P.Y. Yu, M. Cardona. *Fundamentals of Semiconductors: Physics and Materials Properties* (Springer, Berlin, 2010). DOI: 10.1007/978-3-642-00710-1

[14] J.K. Chena, D.Y. Tzou, J.E. Beraun. Int. J. Mass Heat Transfer, **49**, 307 (2006). DOI: 10.1016/j.ijheatmasstransfer.2005.06.022

[15] P.I. Lazarenko, Yu.V. Vorobyov, M.E. Fedyanina, A.A. Sherchenkov, S.A. Kozyukhin, A.O. Yakubov, A.V. Kukin, Yu.S. Sybina, I.V. Sagunova. Inorg. Mater. Appl. Res., **11**, 330 (2020). DOI: 10.1134/S2075113320020227

[16] S. Liu, J. Wei, F. Gan. J. Appl. Phys., **110** (3), 033503 (2011). DOI: 10.1063/1.3614501

[17] L.E. Shelimova, O.G. Karpinskii, P.P. Konstantinov, M.A. Kretova, E.S. Avilov, V.S. Zemskov. Inorganic Materials, **37** (4), 342 (2001). DOI: 10.1023/A:1017519625907

[18] S.H. M/oller, E.H. Eriksen, P.L. T/onning, P.B. Jensen., J. Chevallier, P. Balling. Appl. Surf. Sci., **476**, 221 (2019). DOI: 10.1016/j.apsusc.2019.01.070

[19] P. Němec, V. Nazabal, A. Moreac, J. Gutwirth, L. Beneš, M. Frumar. Materials Chemistry and Physics, **136**, 935 (2012). DOI: 10.1016/j.matchemphys.2012.08.024

[20] Z. Xu, C. Chen, Z. Wang, K. Wu, H. Chong, H. Ye. RSC Advances, **8** (37), 21040 (2018). DOI: 10.1039/C8RA01382A

[21] K. Shportko, L. Revutska, O. Paiuk, J. Baran, A. Stronski, A. Gubanova, E. Venger. Optical Materials, **73**, 489 (2017). DOI: 10.1016/j.optmat.2017.08.042

[22] S. Zabotnov, A. Kolchin, D. Shuleiko, D. Presnov, T. Kaminskaya, P. Lazarenko, V. Glukhenkaya, T. Kunkel, S. Kozyukhin, P. Kashkarov. Micro, **2** (1), 88 (2022). DOI: 10.3390/micro2010005

[23] W.Zhou, Z. Zhang, Q. Zhang, D. Qi, T. Xu, S. Dai, X. Shen. Micromachines, **12**, 616 (2021). DOI: 10.3390/mi12060616

[24] J.-L. Battaglia, A. Kusiak, V. Schick, A. Cappella, C. Wiemer, M. Longo, E. Varesi. J. Appl. Phys., **107**, 044314 (2010). DOI: 10.1063/1.3284084

[25] A. Shamova, G. Shandybina, E. Yakovlev, A. Georgieva. Optical Quantum Electron., **49**, 74 (2017). DOI: 10.1007/s11082-017-0911-0